J. Fluid Mech. (1981), *vol.* 109, *pp.* 483–501
Printed in Great Britain

The excitation of Tollmien–Schlichting waves in low subsonic boundary layers by free-stream sound waves

By CHRISTOPHER K. W. TAM

Department of Mathematics and Computer Science, Florida State University, Tallahassee, Florida 32306

(Received 1 December 1978 and in revised form 24 November 1980)

The excitation of Tollmien–Schlichting waves in low subsonic flat-plate boundary layers by sound is investigated theoretically. The problem is formulated mathematically as an inhomogeneous boundary-value problem which is then solved by a Green's-function technique. It is found that the amplitude of the excited Tollmien–Schlichting wave satisfies an inhomogeneous first-order differential equation. The calculated wave amplitude according to this equation exhibits spatial oscillations in the region ahead of the lower branch neutral stable point of the boundary layer. This characteristic feature resembles that observed experimentally by Shapiro (1977). The theoretical value of the coupling constant between incident sound wave and excited Tollmien–Schlichting wave agrees favourably with measured data. Other predictions of the theory also seem to compare well with available experimental measurements.

1. Introduction

Spangler & Wells (1968) and Knapp & Roache (1968) have shown experimentally that sound waves are an important contributing factor to early transition in wind-tunnel boundary-layer flows. It is generally believed that the observed early transition is the consequence of a sequence of events beginning with the excitation of unstable Tollmien–Schlichting waves by the imposed sound fields. The excited Tollmien–Schlichting waves amplify rapidly as they propagate downstream. When these waves attain sufficiently large amplitudes, 'breakdown' occurs which eventually leads to turbulence. (The process of 'breakdown' are very complicated. A new feature involving turbulent spots and Tollmien–Schlichting waves has recently been observed by Wygnanski, Haritonidis & Kaplan (1979).) This paper treats the first part of this early transition process, namely the excitation of Tollmien–Schlichting waves in low subsonic boundary-layer flows by acoustic disturbances.

Classical hydrodynamic stability theory has largely overlooked the acoustic receptivity problem under consideration. Serious investigations began only in the last few years. The first theoretical treatment was published by Mack (1975) for the case of supersonic flow. Mack developed his theory mainly for the purpose of explaining and providing a reasonable estimate of the experimental observations of Kendall (1975) who studied the growth of supersonic boundary-layer instability waves in a wind tunnel. Unfortunately, Mack's pioneering work is not applicable to subsonic flows. Furthermore, the forced excitation of instability waves was ignored in this work. In a

recent review article on boundary-layer stability and transition, Reshotko (1976) briefly discussed various aspects of this problem as well as Mack's theory. It was pointed out that receptivity phenomena of this kind differed physically and mathematically from the usual stability problem. The mathematical problem involved can no longer be formulated as an eigenvalue or normal-mode problem as in classical hydrodynamic-stability theory. Instead, the solution of an inhomogeneous boundary-value problem which describes the forced excitation of instability waves must be sought. A way of solving the inhomogeneous boundary-value receptivity problem was developed recently by the present author, Tam (1978), in connection with the excitation of instability waves in two-dimensional shear layers by sound. In this work the coupling constants between incident sound waves and excited instability waves over the whole range of unstable frequencies were calculated. It was shown how these coupling constants can be used to determine the amplitudes of induced instability waves under the influence of arbitrary incident sound fields. There are, however, two major differences between the acoustic receptivity problem for free shear flows and that for boundary layers. The first important difference arises because of the very distinct roles played by viscosity in the instabilities of these two classes of flows. At moderately high Reynolds number, viscosity is non-essential to the instability of free shear flows. For stability consideration an inviscid analysis is generally regarded as adequate. Experimentally the results of inviscid theory have been found to be valid by Michalke (1965) and Freymuth (1966). On the other hand, it is well known that, contrary to common experience, viscosity is a destabilizing agent in laminar boundary-layer flows (see Lin 1966). In other words, unstable Tollmien–Schlichting waves exist solely because of viscosity. Thus for the boundary-layer acoustic receptivity phenomenon the interaction between nearly inviscid sound waves and viscous Tollmien–Schlichting waves throughout the flow must be accounted for in the formulation of the mathematical problem; whereas in the case of free shear flows a completely inviscid analysis will suffice. The second crucial difference lies in the presence of a solid wall in boundary-layer flows. Because of the wall all the incident sound waves are reflected back so that the physical problem is restricted to a semi-infinite domain. In contrast to this, when a beam of sound waves is aimed at a two-dimensional shear layer only a part of it is being reflected. A sizeable portion of the acoustic waves is transmitted through the layer. The domain of the problem is, therefore, infinite, requiring the prescription of outgoing or boundedness condition far away from the shear layer in all directions. In this paper the receptivity problem for boundary-layer flows will be formulated mathematically in § 2. To solve the inhomogeneous boundary-value problem, however, the method developed in our recent work will be used.

Experimental study of acoustic receptivity characteristics of boundary layers is extremely difficult to perform. Among other things, the requirement of a controlled acoustic environment with only low levels of noise and free-stream turbulence and the near absence of standing acoustic waves in the test section is not easily attainable in a wind tunnel. In addition, possible flow separation near the leading edge of the plate and early transition induced by side-wall turbulent boundary layers must be avoided. Recently, using a wind tunnel specifically designed to minimize these problems, Shapiro (1977) carefully carried out a series of acoustic receptivity measurements. These measurements were intended to shed light on possible excitation of Tollmien–

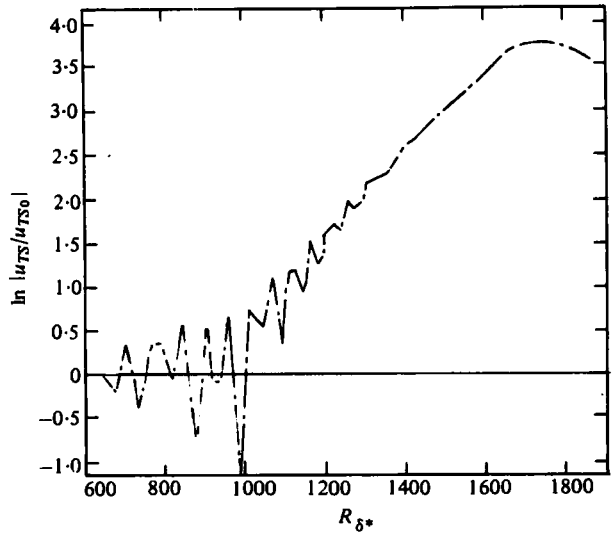

FIGURE 1. Spatial variation of measured wave amplitude, after Shapiro (1977). $\beta = 56 \times 10^{-6}$, $M = 0{\cdot}0845$, incident sound wave at 97 dB SPL.

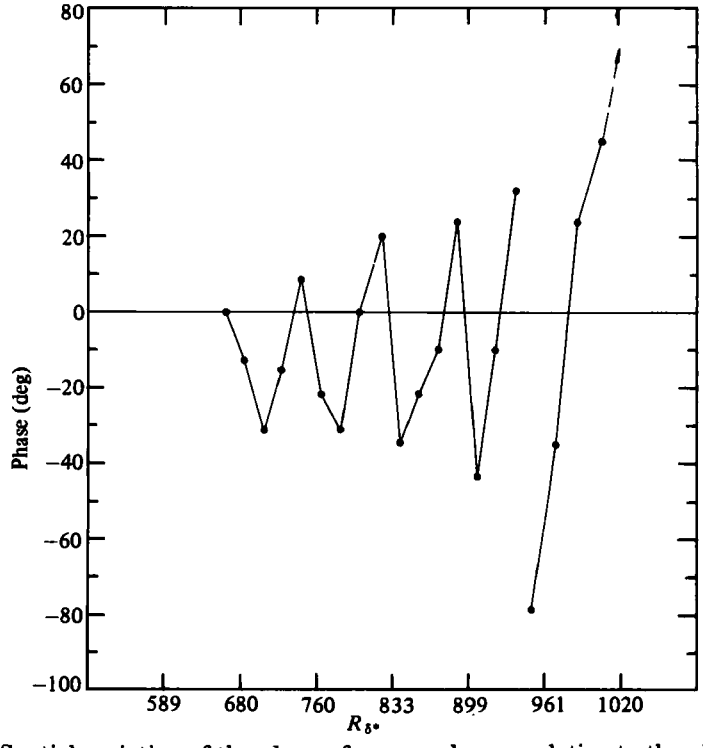

FIGURE 2. Spatial variation of the phase of measured wave relative to the phase of the driving sine wave, after Shapiro (1977).

Schlichting waves and to study the characteristics of these waves under acoustic forcing. A flat-plate boundary layer forced by sound waves propagating in the direction of the free stream was employed in the experiment. Unfortunately, the experimental results did not reveal the mechanism by which the sound waves were coupled to the instability waves of the flow. Yet the excited Tollmien–Schlichting waves did acquire sufficiently large amplitudes to be measured and analysed. On the basis of his experimental results Shapiro found several important characteristics of the excitation process. Firstly, the measured disturbance amplitude (velocity component in the direction of free stream) exhibited spatial oscillation in a broad region of the boundary layer near the location which corresponded to the lower branch of the neutral stability curve. This is shown in figure 1. The wavelength of the spatial oscillations was approximately equal to the local Tollmien–Schlichting wavelength. In the region ahead of the neutral stable point, the phase of the measured velocity component also underwent spatial oscillations with similar wavelength as the amplitude. Figure 2 shows the actual measured data when the imposed sound level was 97 dB SPL at a frequency of 500 Hz. Beyond the neutral stable point the phase appeared to increase essentially linearly with distance but with superimposed small-amplitude oscillations. Secondly, the spatial average of the velocity fluctuations in the region ahead of the neutral stable point (this is the value U_{TS0} in figure 1) was observed to be nearly constant and was approximately equal to the velocity of the incident sound field. Although a closer examination would probably be required before this observation can be used to estimate mate the coupling constant between sound and Tollmien–Schlichting waves yet it does give a very useful measure of the strength of the type of interaction under consideration. Thirdly, when the excited Tollmien–Schlichting wave amplitude was sufficiently large the measured growth rate matched the theoretical predictions of the Orr–Sommerfeld equation (the eigenvalues). In addition, the measured (velocity) amplitude distribution of the disturbance agreed quite well with the predicted eigenfunctions. This offered concrete evidence that the excited disturbances were induced Tollmien–Schlichting waves.

In this paper the boundary-layer acoustic receptivity problem will be formulated in § 2. The problem considered there is identical to Shapiro's experiment, that is, a flat-plate boundary layer forced by plane acoustic waves propagating in the direction of the free-stream flow. This is done so as to allow a direct comparison between the present theory and Shapiro's observations. A general formulation of the receptivity problem can, however, be carried out in a straightforward manner following the same procedure. The solution of the receptivity problem is given in § 3 where it is found that the forced Tollmien–Schlichting wave amplitude satisfies a complex wave amplitude equation. In the absence of forcing, this equation yields solutions which are the same as those of the classical hydrodynamic stability theory. Comparisons between numerical results and experiments are carried out in § 4. It must be pointed out that, despite the extremely careful precautions taken, a very large static pressure gradient existed near the leading edge of the flat plate in Shapiro's experiment. In addition, in the region ahead of the lower neutral stable point the flow was subjected to a moderate destabilizing pressure gradient. Unfortunately Shapiro did not provide any measured mean flow profile in his report to allow this pressure gradient to be taken into consideration in the calculation. A Blasius flow is, therefore, assumed in the theory. This difference between the theoretical model and the experimental condition must be kept in mind

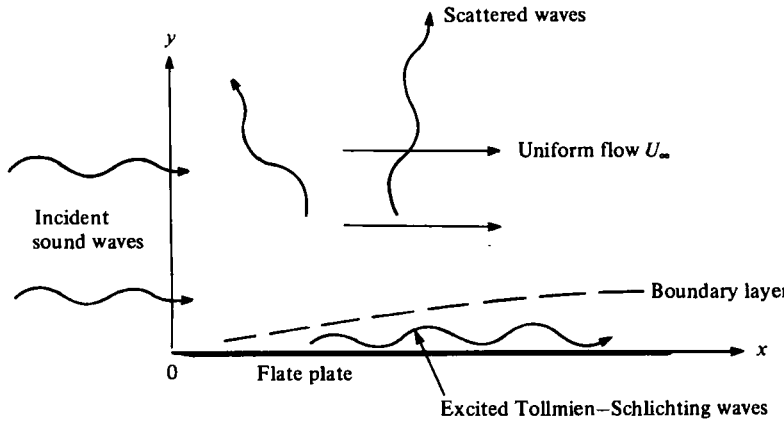

FIGURE 3. Schematic diagram showing boundary-layer flow under the forcing of plane acoustic waves propagating in the direction of the free stream.

when comparing theory with Shapiro's measurements. Overall favourable agreement is found. In §5, the coupling mechanism between incident sound wave and Tollmien–Schlichting wave will be analysed within the framework of the present theory. Other interpretation of Shapiro's data will also be discussed and compared with the present work.

2. Formulation

Consider a flat-plate boundary layer excited by plane sound waves propagating in the direction of the free stream as shown in figure 3. The sound wave has a small amplitude so that in the free stream it is given by the solution of the linearized compressible flow equations. Let $\rho, p, (u, v)$ with subscript i denote the density, pressure and velocity components associated with the incident sound wave; then, by solving the linearized equations of motion, it is straightforward to find that such a plane acoustic wave with frequency Ω and velocity amplitude u_∞ is given approximately by

$$\begin{Bmatrix} u_i \\ p_i \\ \rho_i \end{Bmatrix} = \begin{Bmatrix} u_\infty \\ \gamma M p_\infty \\ M\rho_\infty \end{Bmatrix} \exp\left[i\left(\frac{x}{a_\infty + u_\infty} - t\right)\Omega\right], \tag{2.1}$$

where a_∞ is the speed of sound in the free stream and $M = u_\infty/a_\infty$ is the flow Mach number. In deriving the expression of equation (2.1) the effect of viscous damping which is insignificant in the present context has been ignored. For an incident acoustic wave with amplitude u_s the corresponding velocity, pressure and density fluctuations will be equal to ϵ times that given in equation (2.1) where $\epsilon = u_s/u_\infty$.

Now consider the boundary-layer flow adjacent to the flat plate. The governing compressible flow equations are

$$\frac{\partial \rho}{\partial t} + \frac{\partial \rho u}{\partial x} + \frac{\partial \rho v}{\partial y} = 0, \tag{2.2a}$$

$$\rho\left(\frac{\partial u}{\partial t} + u\frac{\partial u}{\partial x} + v\frac{\partial u}{\partial y}\right) = -\frac{\partial p}{\partial x} + \mu\left(\frac{\partial^2 u}{\partial x^2} + \frac{\partial^2 u}{\partial y^2}\right), \tag{2.2b}$$

$$\rho\left(\frac{\partial v}{\partial t}+u\frac{\partial v}{\partial x}+v\frac{\partial v}{\partial y}\right)=-\frac{\partial p}{\partial y}+\mu\left(\frac{\partial^2 v}{\partial x^2}+\frac{\partial^2 v}{\partial y^2}\right), \tag{2.2c}$$

$$\frac{\partial p}{\partial t}+\frac{\partial pu}{\partial x}+\frac{\partial pv}{\partial y}+(\gamma-1)\,p\left(\frac{\partial u}{\partial x}+\frac{\partial v}{\partial y}\right)=0. \tag{2.2d}$$

In equation (2.2d), the energy equation, heating due to viscous dissipation and thermal conduction has been neglected. At low subsonic flows these effects are relatively unimportant. The boundary conditions on the flat plate are

$$y=0, \quad u=v=0. \tag{2.3}$$

By means of (2.1) the appropriate boundary conditions far away from the wall are

$$y\to\infty, \quad \begin{Bmatrix} u \\ p \\ \rho \end{Bmatrix} \to \begin{Bmatrix} u_\infty+\epsilon u_i(x,t) \\ p_\infty+\epsilon p_i(x,t) \\ \rho_\infty+\epsilon\rho_i(x,t) \end{Bmatrix} + \text{outgoing scattered waves.} \tag{2.4}$$

The parameter ϵ in equation (2.4), which is the ratio of the maximum sound wave velocity to free-stream velocity, is exceedingly small (e.g. in Shapiro's experiment ϵ is approximately equal to 10^{-4}). It is convenient, therefore, to make use of this fact to look for a solution of the mathematical problem consisting of equations (2.2)–(2.4) in the form of power series in ϵ, that is,

$$u=u_0(x,y)+\epsilon u_1(x,y,t)+\epsilon^2 u_2+\ldots. \tag{2.5}$$

In this paper attention will be limited to the solution up to order ϵ only. By substituting (2.5) into equations (2.2)–(2.4) and upon partitioning terms according to powers of ϵ, it is straightforward to show that the zeroth-order terms, u_0, v_0, p_0 and ρ_0, are just the solution of a steady uniform flow past a flat plate. An approximate solution which is accurate to order $1/R_\delta$, where R_δ is the Reynolds number based on boundary-layer thickness, is the well-known Blasius boundary-layer solution. This solution will be used in this paper. Hence we have $\rho_0=\rho_\infty$, $p_0=p_\infty$ and $u_0(x,y)$ given by the Blasius velocity profile. Upon ignoring terms of order $1/R_\delta$, which is part of the generally accepted locally parallel flow approximation in hydrodynamic stability theory, the governing equations for the first-order quantities (u_1, v_1, p_1, ρ_1) can be obtained in a straightforward manner. The boundary conditions for these first-order quantities are

$$y=0, \quad u_1=v_1=0; \tag{2.6}$$

$$y\to\infty, \quad \begin{Bmatrix} u_1 \\ p_1 \\ \rho_1 \end{Bmatrix} \to \begin{Bmatrix} u_i(x,t) \\ p_i(x,t) \\ \rho_i(x,t) \end{Bmatrix} + \text{outgoing scattered waves.} \tag{2.7}$$

Thus as indicated by boundary condition (2.7) the boundary-value problem for these first-order quantities is inhomogeneous. To facilitate the construction of the first-order solution which will describe the acoustic receptivity phenomenon, a change of dependent variables will be made so that the boundary condition at $y\to\infty$ is homogeneous. Let

$$\begin{aligned} u' &= u_1(x,y,t)-u_i(x,t), \quad v'=v_1(x,y,t), \\ p' &= p_1(x,y,t)-\rho_i(x,t), \quad \rho'=\rho_1(x,y,t)-\rho_i(x,t). \end{aligned} \tag{2.8}$$

By subtracting the governing equations of the incident sound wave, (u_i, p_i, ρ_i) from

those of (u_1, v_1, p_1, ρ_1), the first-order quantities, it is easy to find that the equations for the new variables are

$$\rho_\infty\left(\frac{\partial u'}{\partial t}+u_0\frac{\partial u'}{\partial x}+v'\frac{\partial u_0}{\partial y}\right)+\frac{\partial p'}{\partial x}-\mu\left(\frac{\partial^2 u'}{\partial x^2}+\frac{\partial^2 u'}{\partial y^2}\right)=\rho_\infty(u_\infty-u_0)\frac{\partial u_i}{\partial x}, \tag{2.9a}$$

$$\rho_\infty\left(\frac{\partial v'}{\partial t}+u_0\frac{\partial v'}{\partial x}\right)+\frac{\partial p'}{\partial y}-\mu\left(\frac{\partial^2 v'}{\partial x^2}+\frac{\partial^2 v'}{\partial y^2}\right)=0, \tag{2.9b}$$

$$\frac{\partial p'}{\partial t}+u_0\frac{\partial p'}{\partial x}+\gamma p_\infty\left(\frac{\partial u'}{\partial x}+\frac{\partial v'}{\partial y}\right)=(u_\infty-u_0)\frac{\partial p_i}{\partial x}. \tag{2.9c}$$

The new boundary conditions are

$$y=0, \qquad v'=0, \quad u'(x,o,t)=-u_i(x,t); \tag{2.10), (2.11}$$

$$y\to\infty, \quad \text{solution satisfies boundedness or outgoing wave condition.} \tag{2.12}$$

Notice that the inhomogeneous terms of equation (2.9) vanish outside the boundary layer. They represent distributed sources throughout the boundary layer which are responsible for exciting the Tollmien–Schlichting waves. The inhomogeneous boundary-value problem, (2.9)–(2.12), has now been cast into a form typical of most wave-scattering problems arising from volume and surface inhomogeneities. This mathematical problem will be solved in the next section.

3. The Green's function and the wave amplitude equation

To solve the inhomogeneous boundary-value problem (2.9)–(2.12) the locally parallel flow approximation widely used in hydrodynamic stability calculation will be adopted. In this approximation the local growth of the boundary layer is neglected. In other words, $L=(xu/u_\infty)^{\frac{1}{2}}$, the local length scale of the boundary layer, is assumed to be a constant. It must be remembered, however, that the inhomogeneous terms of equations (2.9) and (2.11) are functions of the streamwise co-ordinate. The overall variation of these functions in the free-stream direction should not be ignored. To account for this streamwise dependence, we will follow the technique used in our previous work (Tam 1978) which consists of first constructing a local Green's function. The Green's function satisfies the same inhomogeneous boundary-value problem as (2.9)–(2.12) except that the factor $\exp[ix\Omega/(a_\infty+u_\infty)]$ of the inhomogeneous terms is replaced by a delta function. In terms of dimensionless variables,

$$\left.\begin{aligned}&\xi=x/L, \quad \eta=y/L, \quad \tau=tu_\infty/L, \quad \bar{u}(y)=u_0/u_\infty,\\ &p=p'/\rho_\infty u_\infty^2, \quad u=u'/u_\infty, \quad v=v'/u_\infty,\\ &R=u_\infty L/\nu, \quad \bar{\Omega}=\Omega L/u_\infty, \quad M=u_\infty/a_\infty\end{aligned}\right\} \tag{3.1}$$

($L=(x\nu/u_\infty)^{\frac{1}{2}}$ is the local length scale), the Green's function (denoted by a subscript g) is given by the solution of the mathematical problem below:

$$\frac{\partial u_g}{\partial\tau}+\bar{u}\frac{\partial u_g}{\partial\xi}+v_g\frac{d\bar{u}}{d\eta}+\frac{\partial p_g}{\partial\xi}-\frac{1}{R}\left(\frac{\partial^2 u_g}{\partial\xi^2}+\frac{\partial^2 u_g}{\partial\eta^2}\right)=(1-\bar{u})\frac{\partial\delta(\xi-\zeta)}{\partial\xi}e^{-i\bar{\Omega}\tau}, \tag{3.2a}$$

$$\frac{\partial v_g}{\partial\tau}+\bar{u}\frac{\partial v_g}{\partial\xi}+\frac{\partial p_g}{\partial\eta}-\frac{1}{R}\left(\frac{\partial^2 v_g}{\partial\xi^2}+\frac{\partial^2 v_g}{\partial\eta^2}\right)=0, \tag{3.2b}$$

$$M^2\left(\frac{\partial p_g}{\partial \tau}+\bar{u}\frac{\partial p_g}{\partial \xi}\right)+\frac{\partial u_g}{\partial \xi}+\frac{\partial v_g}{\partial \eta}=M(1-\bar{u})\frac{\partial \delta(\xi-\zeta)}{\partial \xi}e^{-i\bar{\Omega}\tau}; \tag{3.2c}$$

at $\eta=0$, $$v_g=0 \tag{3.3}$$

and $$u_g=-\delta(\xi-\zeta)e^{-i\bar{\Omega}\tau}; \tag{3.4}$$

as $\eta\to\infty$, the solution satisfies boundedness or radiation condition. (3.5)

It can easily be verified that $u(\xi,\eta,\tau)$ is related to the Green's function $u_g(\xi,\eta,\tau;\zeta)$ by

$$u(\xi,\eta,\tau)=\int_{-\infty}^{\infty}u_g(\xi,\eta,\tau;\zeta)\,e^{i\zeta\Omega M/(1+M)}d\zeta. \tag{3.6}$$

Also $v(\xi,\eta,\tau)$ and $v_g(\xi,\eta,\tau;\zeta)$, $p(\xi,\eta,\tau;\zeta)$ and $p_g(\xi,\eta,\tau;\zeta)$ are similarly related. Thus once the Green's function is found the local response of the boundary layer to acoustic excitation can be readily determined.

3.1. *The Green's function*

Let $\tilde{f}(k,\omega)$ be the Fourier–Laplace transform of $f(\xi,\tau)$. These Fourier–Laplace transform pairs possess the following integral relationship:

$$f(\xi,\tau)=\int_{\Gamma}\int_{-\infty}^{\infty}\tilde{f}(k,\omega)\,e^{i(k\xi-\omega\tau)}dk\,d\omega, \tag{3.7a}$$

$$\tilde{f}(k,\omega)=\frac{1}{(2\pi)^2}\int_{-\infty}^{\infty}\int_{0}^{\infty}f(\xi,\tau)\,e^{-i(k\xi-\omega\tau)}d\tau\,d\xi. \tag{3.7b}$$

In (3.7a) the inverse integration contour Γ is taken to be a line parallel to the real axis in the ω-plane above all singularities of the integrand. By taking the Fourier–Laplace transform of (3.2)–(3.5) and on eliminating $\tilde{u}_g$, the equations and boundary conditions for $\tilde{p}_g$ and $\tilde{v}_g$ are

$$\frac{d^2\tilde{p}_g}{d\eta^2}-k^2\tilde{p}_g+\frac{1}{1-iM^2(\omega-\bar{u}k)/R}\left\{M^2(\omega-\bar{u}k)^2\tilde{p}_g+i2k\frac{d\bar{u}}{d\eta}\tilde{v}_g+\frac{iM^2k}{R}\left(\frac{d^2\bar{u}}{d\eta^2}\tilde{p}_g+2\frac{d\bar{u}}{d\eta}\frac{d\tilde{p}_g}{d\eta}\right)\right\}$$

$$=\frac{k}{[1-iM^2(\omega-\bar{u}k)/R]}\left\{-ik(1-\bar{u})\left[1+\frac{iMk}{R}+M\left(\frac{\omega}{k}-\bar{u}\right)\right]+\frac{M}{R}\frac{d^2\bar{u}}{d\eta^2}\right\}\frac{e^{-ik\zeta}}{4\pi^2(\omega-\bar{\Omega})}, \tag{3.8a}$$

$$\frac{d^2\tilde{v}_g}{d\eta^2}-[k^2-iR(\omega-\bar{u}k)]\tilde{v}_g-R\frac{d\tilde{p}_g}{d\eta}=0; \tag{3.8b}$$

at $\eta=0$, $$\tilde{v}_g=0 \tag{3.9}$$

and $$\frac{d\tilde{v}_g}{d\eta}-iM^2\omega\tilde{p}_g=-(1+M)\frac{ke^{-ik\zeta}}{4\pi^2(\omega-\bar{\Omega})}; \tag{3.10}$$

as $\eta\to\infty$, the solution satisfies boundedness or radiation condition. (3.11)

After $\tilde{p}_g$ and $\tilde{v}_g$ are found, $\tilde{u}_g$ can be found in terms of those functions through the

transform of equation (3.2*c*). A system of inhomogeneous ordinary differential equations such as equation (3.8) possesses homogeneous and particular solutions. Let

$$\begin{pmatrix}\tilde{p}_g\\ \tilde{v}_g\end{pmatrix} = \begin{pmatrix}\phi_p(\eta,k,\omega)\\ \phi_v(\eta,k,\omega)\end{pmatrix} \quad \text{and} \quad \begin{pmatrix}\chi_p(\eta,k,\omega)\\ \chi_v(\eta,k,\omega)\end{pmatrix} \tag{3.12}$$

be two linearly independent homogeneous solutions and

$$\begin{pmatrix}\tilde{p}_g\\ \tilde{v}_g\end{pmatrix} = \frac{e^{-ik\zeta}}{4\pi^2(\omega-\bar{\Omega})}\begin{pmatrix}\tilde{p}_s(\eta,k,\omega)\\ \tilde{v}_s(\eta,k,\omega)\end{pmatrix} \tag{3.13}$$

be a particular solution of (3.8) satisfying boundary condition (3.11). Then the solution of the inhomogeneous boundary-value problem (3.8)–(3.11) can be written as

$$\begin{pmatrix}\tilde{p}_g(\eta,k,\omega;\zeta)\\ \tilde{v}_g(\eta,k,\omega;\zeta)\end{pmatrix} = D\begin{pmatrix}\phi_p(\eta,k,\omega)\\ \phi_v(\eta,k,\omega)\end{pmatrix} + F\begin{pmatrix}\chi_p(\eta,k,\omega)\\ \chi_v(\eta,k,\omega)\end{pmatrix} + \frac{e^{-ik\zeta}}{4\pi^2(\omega-\bar{\Omega})}\begin{pmatrix}\tilde{p}_s(\eta,k,\omega)\\ \tilde{v}_s(\eta,k,\omega)\end{pmatrix}, \tag{3.14}$$

where the constants D and F are determined by using boundary conditions (3.9) and (3.10). By means of (3.14) and the transform of (3.2*c*) a formula for $\tilde{u}_g$ can be established after some algebraic manipulations. The denominator of this formula involves a factor $\Delta(k,\omega)$ which is given by

$$\Delta(k,\omega) \equiv \left[\phi_v\left(\frac{d\chi_v}{d\eta} - iM^2\omega\chi_p\right) - \chi_v\left(\frac{d\phi_v}{d\eta} - iM^2\omega\phi_p\right)\right]_{\eta=0}. \tag{3.15}$$

It is noted that $\Delta(k,\omega) = 0$ is the dispersion function of the Tollmien–Schlichting waves. Now the Green's function $u_g(\xi,\eta,\tau;\zeta)$ can be constructed by taking the inverse transform of $\tilde{u}_g$, namely

$$u_g(\xi,\eta,\tau;\zeta) = \int_\Gamma\int_{-\infty}^{\infty} \tilde{u}_g(\eta,k,\omega;\zeta)\exp\left[i(k\xi-\omega\tau)\right]dk\,d\omega. \tag{3.16}$$

Equation (3.16) gives the total local response of the boundary layer subjected to acoustic excitation. Here we are only interested in the part of the response directly related to the Tollmien–Schlichting waves. This arises from certain poles of the integrand in the ω and the k planes. To evaluate the double integral of (3.16) we will follow the procedure of Briggs (1964, chap. 2). This procedure has been used by the present author in connection with the generation of jet noise by shear-layer instability (Tam 1971) and the excitation of shear-layer instability waves by sound (Tam 1978). To ensure that causality condition is observed, namely, $u_g(\xi,\eta,\tau;\zeta)\to 0$ as $\tau\to-\infty$, the inverse contour Γ is first put in the upper half ω-plane with $\mathrm{Im}(\omega)\to\infty$. This step assures that Γ is above all singularities of the integrand. Since ω is a value of Γ, one can solve for the roots $k(\omega)$ of $\Delta(k,\omega_r+i\infty)=0$ and determine the relative positions of the poles of the integrand and the inverse contour in the k-plane. Now the contour Γ is deformed towards the real axis in the ω-plane as illustrated in figure 4. As a result, the roots $k(\omega)$ or the poles of the integrand of (3.16) move about in the k-plane. In the case of instability, a pole which originates in the upper half k-plane would cross the real k axis into the lower half-plane during this process of contour deformation. Figure 4 depicts the movement of the unstable Tollmien–Schlichting wave pole $k_+(\omega)$ for the case $R_{\delta^*}=1200, f=500$ Hz and $u_\infty = 28\,\mathrm{m\,s^{-1}}$ where R_{δ^*} is the Reynolds number based on displacement thickness, f is the wave frequency and u_∞ is the free-stream flow velocity (these are the values used in Shapiro's experiment). For spatially damped waves the corresponding pole in the k-plane would not cross the real axis. The acoustically

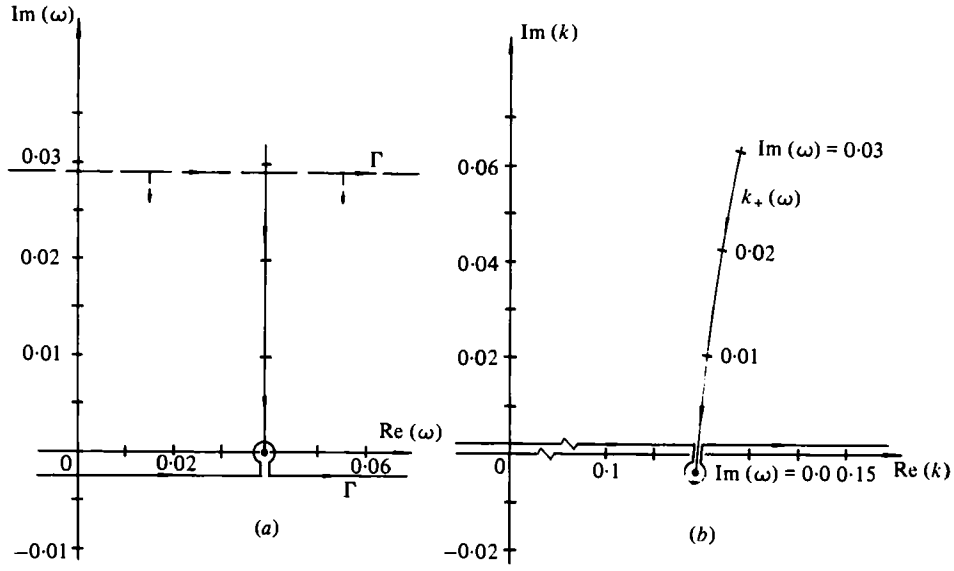

FIGURE 4. Movement of $k_+(\omega)$ pole as ω of Γ contour is pushed towards the real axis along the line Re $(\omega) = 0{\cdot}03905$ which corresponds to $f = 500$ Hz at $u_\infty = 29$ m s^{-1}, $R_{\delta^*} = 1200$. (*a*) ω-plane, (*b*) k-plane.

excited Tollmien–Schlichting wave is given by the residue contributions of the pole $\omega = \bar{\Omega}$ in the ω-plane and the pole $k = k_+(\bar{\Omega})$ in the k-plane where $\Delta(k_+(\bar{\Omega}), \bar{\Omega}) = 0$. The unsteady acoustic boundary layer or in the limit of incompressible flow the Stokes shear wave which represents a well-known component of the response of the boundary layer to the imposed sound wave is given by the remaining part of the integral over the deformed contour. Ignoring this contribution to the integrals or keeping only the excited Tollmien–Schlichting wave solution it is straightforward to find from (3.15) and (3.16) the following formula for the Green's function:

$$u_g(\xi, \eta, \tau; \zeta) = \sigma \hat{u}(\eta, k_+, \bar{\Omega}) \exp\left(ik_+(\xi - \zeta) - i\bar{\Omega}\tau\right) H(\xi - \zeta), \tag{3.17}$$

where σ, the coupling constant, is a function of M, $\bar{\Omega}$ and R_{δ^*} and $\hat{u}(\eta, k_+, \bar{\Omega})$ is the normalized eigenfunction of the Tollmien–Schlichting wave and $H(\xi - \zeta)$ is the unit step function. They are given by

$$\sigma = \left\{1 + M + \frac{1}{k_+}\left[\frac{d\tilde{v}_s}{d\eta} - iM^2\bar{\Omega}\tilde{p}_s - \frac{\tilde{v}_s}{\chi_v}\left(\frac{d\chi_v}{d\eta} - iM^2\bar{\Omega}\chi_p\right)\right]\right\}_{\eta=0} \frac{E}{(\partial\Delta/\partial k)_{k_+,\bar{\Omega}}}, \tag{3.18}$$

$$\hat{u}(\eta, k_+, \bar{\Omega}) = \frac{1}{E}\left[\chi_v(\eta = 0)\left(i\frac{d\phi_v}{d\eta} + M^2(\omega - \bar{u}k_+)\,\phi_p\right) - \phi_v(\eta = 0)\left(i\frac{d\chi_v}{d\eta} + M^2(\omega - \bar{u}k_+)\,\chi_p\right)\right], \tag{3.19}$$

$$H(\xi - \zeta) = \begin{cases} 0, & \xi < \zeta; \\ 1, & \xi > \zeta. \end{cases}$$

The constant E is chosen so that $\hat{u}(\eta, k_+, \bar{\Omega})$ satisfies the normalization condition

$$\int_0^\infty \left[\tfrac{1}{4}\bar{u}(|\hat{u}|^2 + |\hat{v}|^2) + \tfrac{1}{2}\,\mathrm{Re}\,(\hat{p}\hat{u}^*)\right] d\eta = 1, \tag{3.20}$$

where $\hat{u}^*$ is the complex conjugate of $\hat{u}$.

3.2. *The wave amplitude equation*

By means of the Green's function (3.17) and equation (3.6) we find

$$\frac{u'(\xi,\eta,\tau)}{u_\infty} = \sigma\left[\int_{-\infty}^{\xi} \exp\left(\frac{iM\bar{\Omega}\zeta}{1+M} + ik_+(\xi-\zeta) - i\bar{\Omega}\tau\right) d\zeta\right] \hat{u}(\eta, k_+, \bar{\Omega}). \tag{3.21}$$

Let the x-velocity component of the excited Tollmien–Schlichting wave be u_{TS}. This quantity, which is measurable experimentally, can be found by substituting (3.21) into (2.8) and then into (2.5):

$$\frac{u_{TS}}{u_s} = \sigma\left[\int_{-\infty}^{\xi} \exp\left(\frac{iM\bar{\Omega}\zeta}{1+M} + ik_+(\xi-\zeta) - i\bar{\Omega}\tau\right) d\zeta\right] \hat{u}(\eta, k_+, \bar{\Omega}). \tag{3.22}$$

In (3.22) u_s is the velocity of the incident acoustic wave. We will define the amplitude of the excited Tollmien–Schlichting wave, A, by

$$u_{TS} \equiv A\hat{u}(\eta, k_+, \bar{\Omega})\, e^{-i\bar{\Omega}\tau} = A\hat{u}(\eta, k_+, \bar{\Omega})\, e^{-i\Omega t}. \tag{3.23}$$

In (3.22) the physical variable which is of special interest to us, is the streamwise distribution of wave amplitude A. To determine this amplitude function we will first substitute (3.23) into (3.22) and then differentiate the equation with respect to ξ. Upon dividing out the common factor $\hat{u}(\eta, k_+, \bar{\Omega}) \exp(-i\Omega t)$, the following equation for A can be derived,

$$dA/d\xi = ik_+(\bar{\Omega})\, A + \sigma u_s\, e^{iM\bar{\Omega}\xi/(1+M)}.$$

Now, if the co-ordinate variable x is used instead of ξ, the desired wave amplitude equation which describes the spatial evolution of the Tollmien–Schlichting wave amplitude under acoustic forcing is obtained:

$$\frac{dA}{dx} = i\frac{k_+}{L}A + \frac{\sigma u_s}{L}\exp\left[\frac{iM\Omega}{1+M}\frac{x}{u_\infty}\right]. \tag{3.24}$$

In (3.24), $L = (x\nu/u_\infty)^{\frac{1}{2}}$ is the local length scale of the boundary layer. Equation (3.24) is one of the principal results of this work. In the absence of sound, that is $u_s = 0$, this equation gives the local growth rate of the free Tollmien–Schlichting wave mode. An important implication of this wave amplitude equation is that the local growth rate of the forced Tollmien–Schlichting wave is not equal to the imaginary part of (k_+/L) as in the case of free wave mode. The local growth rates of the free and forced modes are approximately equal only when the wave amplitude is very large, that is to say when the first term on the right-hand side of (3.24) is much larger than the second term. This is consistent with Shapiro's (1977) observations and occurs at large R_{δ^*}. The second term on the right-hand side of (3.24) is linearly proportional to the amplitude of the incident acoustic wave. Clearly it represents a forcing term. It is this term which is responsible for the excitation of Tollmien–Schlichting waves in the boundary layer. The quantity σ is a measure of the strength of interaction between incident acoustic wave and excited Tollmien–Schlichting wave. For this reason we have referred to it in (3.17) as the coupling constant.

To find the amplitude of the excited Tollmien–Schlichting wave it is necessary to integrate equation (3.24). In hydrodynamic stability theory, the standard practice (see Mack 1977) which has proved to be valid, is to take into account the variation of boundary-layer thickness by treating the coefficients k_+/L and σ/L no longer as

constants but as functions of x at this stage. Since these coefficients are usually computed as functions of Reynolds number $R = u_\infty L/\nu$ (based on length scale L) or $R_{\delta^*} = 1{\cdot}7028R$ (based on boundary-layer displacement thickness), it is, therefore, more convenient to use R or R_{δ^*} as the independent variable instead of x. In terms of R_{δ^*} the wave amplitude equation becomes

$$\frac{d(A/u_s)}{dR_{\delta^*}} = 1{\cdot}162\left[ik_+\left(\frac{A}{u_s}\right) + \sigma \exp\left[i\frac{M\beta}{1+M}\left(\frac{R_{\delta^*}}{1{\cdot}7208}\right)^2\right]\right]. \tag{3.25}$$

In (3.25) $\beta = \Omega\nu/u_\infty^2$ is the dimensionless frequency parameter. (3.25) is a first-order differential equation. To specify its solution uniquely one initial condition must be imposed on A. This initial condition is not provided by the stability analysis. It has to be motivated by the physics of the overall problem. The most natural initial condition appears to be that which requires the Tollmien–Schlichting wave to start out with zero amplitude somewhere near the leading edge of the flat plate, say, at $R_{\delta^*} = R_0$. This condition will be adopted in this paper. Mathematically, this is expressed as

$$A(R_0) = 0. \tag{3.26}$$

The solution of (3.25) satisfying (3.26) can easily be found by the method of variation of parameters which gives

$$\frac{A(R_{\delta^*})}{u_s} = 1{\cdot}162\exp\left[1{\cdot}162i\int_{R_0}^{R_{\delta^*}} k_+(y)\,dy\right] \times \int_{R_0}^{R_{\delta^*}} \sigma(z)\exp\left[i\frac{M\beta}{1+M}\left(\frac{z}{1{\cdot}7208}\right)^2 - 1{\cdot}162i\int_{R_0}^{z} k_+(z')dz'\right]dz. \tag{3.27}$$

Equation (3.27) provides a complete description of the spatial evolution of the excited Tollmien–Schlichting wave amplitude. It will be used to compare with experimental measurements in the following section.

4. Numerical results and comparison with experiment

At low subsonic Mach number the boundary-layer flow over a flat plate has a Blasius velocity profile. This mean velocity profile is used in all the stability calculations of this paper. The first step towards computing the spatial evolution of the amplitude of the excited Tollmien–Schlichting wave is to construct the two linearly independent homogeneous solutions, (3.12), and the particular solution, (3.13), of equation (3.8) numerically. For this purpose, a number of methods have been discussed by various authors in the literature. Throughout this work, the method of orthonormalization is employed. An excellent exposition of this method was recently given by Scott & Watts (1977). By means of orthonormalization, two linearly independent homogeneous solutions of equation (3.8) satisfying condition (3.14) were computed by the Runge–Kutta–Gill numerical integration algorithm. We started the solutions at a distance of $8L$ ($L = (x\nu/u_\infty)^{\frac{1}{2}}$ is the local length scale) from the wall and integrated into the boundary layer until the wall was reached. A Newton's iteration scheme was used in conjunction with these homogeneous solutions to determine the roots of the dispersion function $\Delta(k_+(\bar{\Omega}), \bar{\Omega})$ as given by equation (3.15). These roots are the eigenvalues of the Tollmien–Schlichting waves according to the classical normal-mode approach of hydrodynamic stability theory. After the root $k_+(\bar{\Omega})$ was found, the normalized eigen-

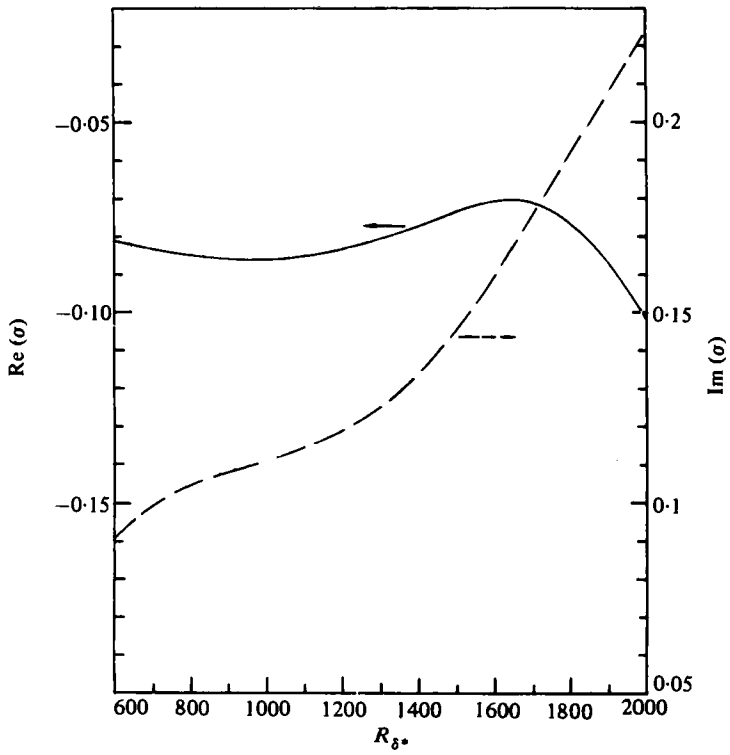

FIGURE 5. Real and imaginary parts of coupling constant σ at $\beta = 56 \times 10^{-6}$.
———, Re (σ); — — — —, Im (σ).

function $\hat{u}(\eta, k_+, \bar{\Omega})$ and the normalization constant E of (3.19) were computed. The particular solution $(\tilde{p}_s, \tilde{v}_s)$ which is needed in calculating the coupling constant σ by equation (3.18) was obtained by numerical integration using the orthonormalization procedure. The inhomogeneous terms of (3.8) are zero outside the boundary layer. This implies that the starting conditions for the particular solution at a distance $8L$ from the wall should be taken to be identically equal to zero. Up to this point the remaining unknown factor required by equation (3.18) is $(\partial\Delta/\partial k)_{k_+,\bar{\Omega}}$. This quantity was calculated by the central difference formula

$$\left(\frac{\partial\Delta}{\partial k}\right)_{k_+,\bar{\Omega}} = \frac{1}{2h}(\Delta(k_+ + h, \bar{\Omega}) - \Delta(k_+ - h, \bar{\Omega})) + O(h^2). \tag{4.1}$$

Equation (4.1) can easily be derived by means of a Taylor series expansion of $\Delta(k, \omega)$ about $(k_+, \bar{\Omega})$ where the function is analytic. In our computation h was assigned to be half a per cent of Re (k_+). This yielded at least a three-figure accuracy in the computed results. Figure 5 shows the values of the real and imaginary parts of the coupling constant σ at $\beta = \Omega\nu/u_\infty^2 = 56 \times 10^{-6}$, $M = 0{\cdot}0845$ (or $f = 500$ Hz and $u_\infty = 20\,\mathrm{m\,s^{-1}}$) for various R_{δ^*}. As can be seen under these conditions the real part of σ is nearly constant over the interval $600 \leqslant \delta^* \leqslant 2000$ while the imaginary part of σ increases in value by a factor of over 2. For convenience, these values of σ were fed into a spline curve computer subroutine program which was used extensively in subsequent calculations.

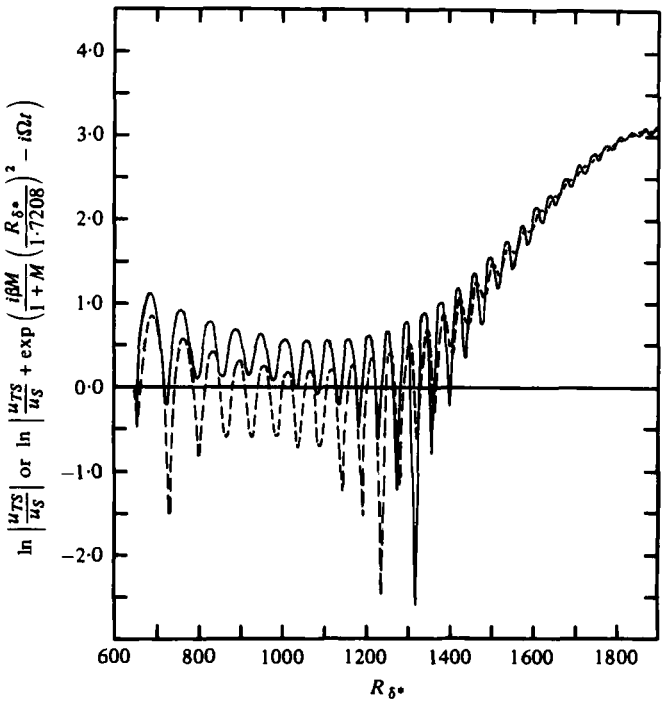

FIGURE 6. Spatial variation of calculated wave amplitude. Initial condition $A = 0$ at $R_{\delta^*} = 650$. $\beta = \Omega\nu/u_\infty^2 = 56 \times 10^{-6}$, $M = u_\infty/a_\infty = 0{\cdot}0845$. ————, Tollmien–Schlichting wave mode alone, $\ln|u_{TS}/u_s|$; — — — —, including acoustic boundary-layer oscillations, equation (4.2).

In §3 the initial condition $A(R_0) = 0$, equation (3.26), was adopted in determining the spatial distribution of excited Tollmien–Schlichting wave amplitude. The value $R_{\delta^*} = R_0$ should correspond to a point of the boundary layer close to the leading edge of the flat plate. Now it must be remembered that the boundary-layer theory which provides the mean flow profile in all our calculation breaks down close to the leading edge of the plate. In addition, the locally parallel flow approximation employed in our stability analysis would certainly be violated in regions very close to the leading edge of the plate. With these constraints in mind we set R_0 equal to 650, which at $\beta = 56 \times 10^{-6}$ corresponds to a point sufficiently far ahead of the lower branch of the neutral stability boundary and at the same time is not too close to the leading edge of the flat plate as to invalidate the assumptions of the theory. We feel that this choice is reasonable. If R_0 is chosen to be somewhat larger than 650, this change in R_0 does not seem to have a significant influence on the calculated results. With $R_0 = 650$ the integrals of equation (3.30) were evaluated numerically. The results are shown in figures 6 and 7. In figure 6 the solid curve gives the logarithm of the absolute value of u_{TS}/u_S (maximized over η) as a function of R_{δ^*}. It is seen that the amplitude, starting from zero at R_0, rises rapidly at first and then undergoes spatial oscillations with wavelength equal to that of the local Tollmien–Schlichting wave. Over the region ahead of the lower branch neutral stable point the spatial average of the amplitude of the excited wave is practically a constant. Downstream of the neutral stable boundary the wave amplitude grows steadily. Small superimposed oscillations can, however, be easily seen. Experimentally, the measured velocity fluctuation, u_{measured}, consists of not only that of the

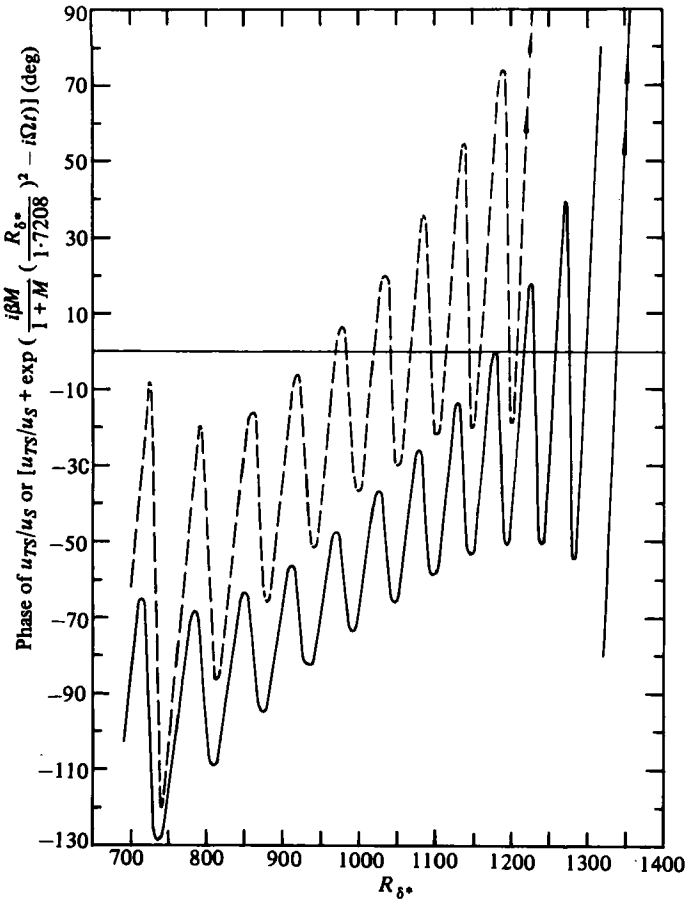

FIGURE 7. Spatial variation of calculated phase of wave relative to the phase of incident sound wave at the leading edge of flat plate. ————, Tollmien–Schlichting wave alone; — — — —, including acoustic boundary-layer oscillations.

Tollmien–Schlichting wave alone. Principally, it is the sum of the excited Tollmien–Schlichting wave and the velocity oscillations of the acoustic boundary layer. At low subsonic Mach number it is given approximately by

$$\left|\frac{u_{\text{measured}}\,(R_{\delta^*},\bar{\eta},t)}{u_s}\right| = \left|\frac{u_{TS}(R_{\delta^*},\bar{\eta})}{u_s} + \exp\left[i\frac{\beta M}{1+M}\left(\frac{R_{\delta^*}}{1{\cdot}7208}\right)^2 - i\Omega t\right]\right|, \tag{4.2}$$

where $|u_{TS}(\eta, k_+, \bar{\Omega})|$ attains its maximum value at $\eta = \bar{\eta}$. The second term on the right-hand side of (4.2) comes from the acoustic wave. The logarithm of this quantity as a function of R_{δ^*} is shown as the dotted curve in figure 6. Notice that the two curves in this figure look qualitatively alike and show striking resemblance to the measured data of Shapiro (1977) in figure 1. Further, in the region ahead of the neutral stable point the averaged value of $|u_{\text{measured}}/u_s|$ of the present calculation is approximately equal to unity. This is also equal to Shapiro's measured value (note: in figure 1 u_{TS0} is equal to u_s according to Shapiro) indicating that the predicted coupling constant σ is, at least, of the right order of magnitude. Figure 7 shows the phase of $u_{TS}(R_{\delta^*},\eta)/u_s$ and $u_{TS}/u_s + \exp[i[\beta M/(1+M)](R_{\delta^*}/1{\cdot}7208)^2 - i\Omega t]$, the measured phase of velocity

fluctuation in the boundary layer, as R_{δ^*} varies. Again these quantities exhibit spatial oscillations in the regions ahead of the neutral stable point with wavelength equal to the local Tollmien–Schlichting wave. This feature is qualitatively the same as that shown in figure 2. The agreement is, however, not as good as that of the absolute amplitude since the calculated phase displays a secular linear increase.

In connection with comparing the present theoretical results with experimental measurements it must be pointed out that despite the extreme precautions taken by Shapiro his data is not completely free of ambiguities. As was mentioned before a large pressure gradient existed near the leading edge of his plate. Also a somewhat mild but unfavourable pressure gradient persisted over the region ahead of the neutral stable point of his flat-plate boundary layer. In addition, there were still a substantial amount of residual noise, turbulence and vibrations in his wind tunnel so that even in his excited case the input disturbance did not consist of sound wave alone. The point here is that receptivity experiments are extremely difficult to perform. In the absence of a set of definitive measurements by which a complete quantitative verification of the theory can be carried out, we believe that the similarities which exist between figures 1 and 6, 2 and 7 do suggest some fairly general agreement between the calculated results and experimental data. Of course, to draw any firm conclusion on the basis of qualitative agreement alone can be misleading. It is worth while to point out, however, that there is one qualitative difference between figures 1 and 6 for small R_{δ^*}. In figure 6 the theoretical curve indicates a slow decay of the average wave amplitude while the experimental curve in figure 1 shows a more or less constant value. One possible reason for this difference is the mild pressure gradient which existed in Shapiro's experiment. This unfavourable pressure gradient tends to destabilize the flow and if accounted for will probably eliminate the small decay of the calculated results. In addition the non-parallel flow effect which has not been included in the present work will also make the boundary layer slightly less stable in this region. It is believed that when all these secondary flow effects are considered the difference can be reconciled.

5. Discussion

The mathematical formulation of the receptivity problem described in this paper is applicable not only to acoustic inputs but to other types of free-stream disturbances such as turbulence and entropy spots as well. For the case of Tollmien–Schlichting waves driven by free-stream turbulence (represented by three-dimensional vorticity waves) in an incompressible boundary layer, the procedure outlined in § 2 leads to the following inhomogeneous boundary-value problem:

$$\rho\left[\frac{\partial}{\partial t}(\nabla^2 v') + u_0\frac{\partial}{\partial x}(\nabla^2 v') - \frac{\partial v'}{\partial x}\frac{\partial^2 u_0}{\partial y^2}\right] - \mu\nabla^4 v' = -\rho(u_0 - u_\infty)\frac{\partial}{\partial x}(\nabla^2 v_t) + \rho\frac{\partial v_t}{\partial x}\frac{\partial^2 u_0}{\partial y^2}.$$

The boundary condition at $y \to \infty$ is

$$v' \to 0.$$

The boundary conditions at $y = 0$ are

$$v' = -v_t(x, 0, z, t), \quad \frac{\partial v'}{\partial y} = -\frac{\partial v_t}{\partial y}(x, 0, z, t).$$

It is to be noted that in this special problem the inhomogeneous terms depend only on v_t, the y-velocity component of the free-stream incident vorticity waves alone. That is

to say, free-stream turbulence can excite unstable Tollmien–Schlichting waves of the boundary layer only through its velocity component in the direction normal to the plate. The streamwise and lateral velocity components have no influence at all. This is a rather unexpected and remarkable result. It is unexpected because clearly in the acoustic receptivity problem the Tollmien–Schlichting wave is driven by the streamwise velocity component of the input sound wave (in the numerical solution the wavelength of sound is so much larger than that of the Tollmien–Schlichting waves that the excitation is effectively caused by free-stream longitudinal velocity oscillations; compressibility effect of the sound waves is unimportant). It is, therefore, natural to expect that the streamwise velocity fluctuations of free-stream turbulence (vorticity waves) should have, at least, some effect in exciting these waves. It is remarkable because the result is so clear-cut and simple that it can easily be tested experimentally. If one uses the wake of a long vibrating ribbon as a source of free-stream turbulence then the vorticity waves generated would have velocity components mainly in the plane normal to the axis of the ribbon. In other words, the vorticity waves are nearly two-dimensional. Now, when such a vibrating ribbon is introduced ahead of a flat plate so that its wake interacts with the boundary layer, two distinctly different conditions can be created. By aligning the axis of the ribbon normal to the plate, the case of boundary-layer flow excited by vorticity waves with negligible velocity component in the normal direction is produced experimentally. On the other hand, by rotating the axis of the ribbon by 90° so that it is parallel to the leading edge of the plate, one finds that the boundary layer is now subjected to free-stream vorticity wave excitation with a substantial velocity component in the normal direction. Notice that in both cases there are streamwise velocity fluctuations in the free stream. Such an experiment was carried out by Kachanov, Kozlov & Levchenko (1978). It was observed that, indeed, when the axis of the vibrating ribbon was normal to the plate little Tolmien–Schlichting wave was detected in the boundary layer, whereas when the axis of the vibrating ribbon was parallel to the leading edge of the plate Tollmien–Schlichting waves were unambiguously found in the boundary-layer flow. Although, again as in the case of acoustic excitation, it is difficult to verify the theory by direct quantitative comparison with experiment at this time (not enough data) yet the agreement between experiment and theory on such a remarkable and unexpected result should not be dismissed lightly. On the contrary, we believe that it does lend strong support to the validity of the present theoretical approach.

Now let us examine the amplitude equation (3.24) again to try to understand in physical terms how Tollmien–Schlichting waves are generated. It is useful here to compare the present situation to that of a vibrating system under the action of external forces. Equation (3.24) is a first-order inhomogeneous ordinary differential equation. As is well known the solution can be regarded as consisting of a particular solution and a homogeneous solution. The former is equivalent to the steady oscillatory solution of a forced vibrating system and the latter is equivalent to the transient solution of the same system. Clearly the homogeneous solution of (3.24) is the classical propagating Tollmien–Schlichting wave mode. The particular solution is a new element introduced in this work. To find an approximate particular solution to (3.24) at low Mach number we note that the two coefficients

$$(\sigma u_s/L)\exp\left[iM\Omega x/(1+M)u_\infty\right] \quad \text{and} \quad ik_+/L$$

are slowly varying functions of x. If these coefficients are independent of x then the particular solution is given by the ratio of these coefficients which again is independent of x. Thus we see that the particular solution represents a form of long-wave oscillations of the whole boundary layer. The amplitude of these oscillations varies very slowly in the streamwise direction. The propagating Tollmien–Schlichting wave mode (homogeneous solution) and the forced Tollmien–Schlichting oscillation (particular solution) are related by initial condition (3.26). This is analogous to the situation of the forced vibrating system where the transient oscillations and forced oscillations are coupled by the initial condition. In this way we see that the forced Tollmien–Schlichting wave oscillation is crucial to the generation of the propagating wave mode. Slightly downstream of the initial point $R_{\delta^*} = R_0$ the superposition of the long-wave mode (particular solution) with nearly constant amplitude and that of the propagating mode (homogeneous solution) produces the characteristic spatial amplitude oscillations shown in figure 6. This feature is unchanged by the inclusion of the incident acoustic wave. For this merely amounts to a small change in the nearly constant amplitude of the Tollmien–Schlichting long-wave mode (particular solution). Finally as the propagating Tollmien–Schlichting wave mode increases in amplitude over the unstable region the amplitude of the Tollmien–Schlichting long-wave mode becomes less and less significant. The overall wave phenomenon, therefore, eventually resembles more and more the characteristics of the classical Tollmien–Schlichting wave as illustrated in figure 6.

In a recent paper, Thomas & Lekoudis (1978) examined Shapiro's data as shown in figures 1 and 2. They presented calculations of the amplitude and phases of a wave pattern consisting of a sound wave and a free Tollmien–Schlichting wave, both of the same frequency, propagating independently. In these calculations the amplitude of the Tollmien–Schlichting wave was assumed to be equal to that of the sound wave at $R_{\delta^*} = 650$ and that there was no phase difference between the two waves at this point. Their computed results, not surprisingly as mentioned above, exhibited characteristic features very similar to those of figures 1 and 2 as well as the present calculated results in figures 6 and 7. Relying on this qualitative agreement alone, they concluded that there was no interaction between the sound wave and Tollmien–Schlichting wave in the boundary layer except possibly at the stagnation point near the leading edge of the plate. In view of our calculated results shown in figures 6 and 7 it is clear that these characteristic spatial amplitude oscillations can also be produced by continuous interaction between the sound and Tollmien–Schlichting waves. There is therefore no basis for their conclusion. Had their proposal of 'no interaction' been meant to refer to the lack of generation of propagating Tollmien–Schlichting wave mode instead, it would have been correct to a large extent as discussed in the preceding paragraph. However, in this case the conclusion is justified not by their calculation but by the present theory.

To conclude, we have presented in this paper a mathematical theory on the receptivity of sound by laminar boundary layer. The calculated results are found to be in fair agreement with all the fragmentary experimental data currently available. Further comparisons between theoretical results and experiment are required in order to demonstrate its complete validity. To this end, it is obvious that a good deal of high-quality experimental measurements is desperately needed at this time.

This work was supported by the National Science Foundation under grant CME78-05122.

REFERENCES

BRIGGS, R. J. 1964 *Electron-Stream Interaction with Plasmas.* Massachusetts Institute of Technology Press.

FREYMUTH, P. 1966 On transition in a separated laminar boundary layer. *J. Fluid Mech.* **25**, 683–704.

KACHANOV, YU. S., KOZLOV, V. V. & LEVCHENKO, V. YA. 1978 Occurrence of Tollmien–Schlichting waves in the boundary layer under the effect of external perturbations. *Izv. Akad. Nauk S.S.S.R. Mekhanika Zhid. i Gaza* (English translation *Fluid Dyn.*) **13**, 704–711.

KENDALL, J. M. 1975 Wind tunnel experiments relating to supersonic and hypersonic boundary layer transition. *A.I.A.A. J.* **13**, 290–299.

KNAPP, C. F. & ROACHE, P. J. 1968 A combined visual and hot-wire anemometer investigation of boundary layer transition. *A.I.A.A. J.* **6**, 29–36.

LIN, C. C. 1966 *Theory of Hydrodynamic Stability.* Cambridge University Press.

MACK, L. M. 1975 Linear stability theory and the problem of supersonic boundary layer transition. *A.I.A.A. J.* **13**, 278–289.

MACK, L. M. 1977 Transition and laminar instability. JPL Publication 77–15.

MICHALKE, A. 1965 On spatially growing disturbances in an inviscid shear layer. *J. Fluid Mech.* **23**, 521–544.

RESHOTKO, E. 1976 Boundary layer stability and transition. *Ann. Rev. Fluid Mech.* **8**, 311–349.

SCOTT, M. R. & WATTS, H. A. 1977 Computational solutions of linear two-point boundary value problems via orthonormalization. *SIAM J. Numer. Anal.* **14**, 40–70.

SHAPIRO, P. 1977 The influence of sound upon laminar boundary layer instability. *Acoustics and Vibration Lab. Rep.* no. 83458–83560–1. Massachusetts Institute of Technology.

SPANGLER, J. G. & WELLS, C. S. 1968 Effect of free stream disturbances on boundary layer transition. *A.I.A.A. J.* **6**, 543–547.

TAM, C. K. W. 1971 Directional acoustic radiation from a supersonic jet generated by shear layer instability. *J. Fluid Mech.* **46**, 757–768.

TAM, C. K. W. 1978 Excitation of instability waves in a two-dimensional shear layer by sound. *J. Fluid Mech.* **89**, 357–371.

THOMAS, A. S. W. & LEKOUDIS, S. G. 1978 Sound and Tollmien–Schlichting waves in a Blasius boundary layer. *Phys. Fluids* **21**, 2112–2113.

WYGNANSKI, I., HARITONIDIS, J. H. & KAPLAN, R. E. 1979 On a Tollmien–Schlichting wave packet produced by a turbulent spot. *J. Fluid Mech.* **92**, 505–528.